Title

THE OBSERVATION OF THE HABIT PLANE SHIFT AND THE MORPHOLOGY OF a"" NITRIDE (Fe16N2) PRECIPITATE IN a-Fe

Author

Shih, Y-C.

Publication Date

1982-06-01

Thesis/dissertation

Lawrence Berkeley Laboratory

UNIVERSITY OF CALIFORNIA

Materials & Molecular Research Division

THE OBSERVATION OF THE HABIT PLANE SHIFT AND THE MORPHOLOGY OF α'' NITRIDE ($Fe_{16}N_2$) PRECIPITATE IN α-Fe

Yih-Cheng Shih
(M.S. thesis)

June 1982

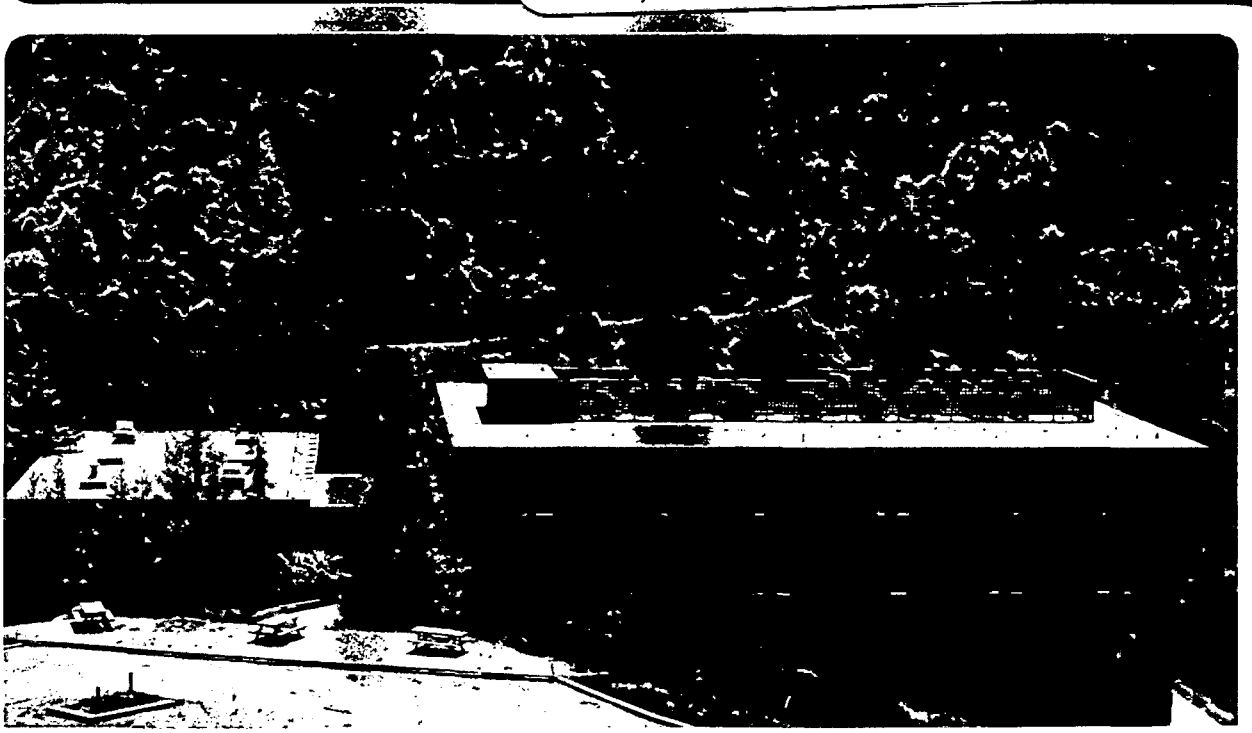

Prepared for the U.S. Department of Energy under Contract DE-AC03-76SF00098

DISCLAIMER

LBL-14284

THE OBSERVATION OF THE HABIT PLANE SHIFT AND THE MORPHOLOGY OF α'' NITRIDE ($Fe_{16}N_2$) PRECIPITATE IN α-Fe

Yih-Cheng Shih

M.S. Thesis

June 1982

Materials and Molecular Research Division
Lawrence Berkeley Laboratory
University of California
Berkeley, CA 94720

This work was supported by the Division of Materials Science, Office of Basic Energy Sciences of the U.S. Department of Energy under Contract No. DE-AC03-76SF00098.

ACKNOWLEDGEMENT

I would like to express my deepest appreciation and gratitude to my advisor, Professor J. W. Morris, Jr. for his guidance and support.

I would also like to thank the members of my group and my department for the many interesting discussions. Special thanks are given to Professor D. Whittle and Dr. R. Gronsky for their review of this manuscript and stimulating discussions. Thanks are also due to Dr. U. Dahmen for his helpful discussions of TEM technique and theory, and to Professor R. Wenk for the use of the JEOL 100C TEM.

I am also grateful to Mrs. Jeanne L. Shull for her delicate preparation of this manuscript, and to Ms. Mariko Kubik for her careful typing.

Finally, I would like to thank my family especially my parents and my wife, Chai Lan, for their unwavering love and support.

This work was supported by the Division of Materials Science, Office of Basic Energy Science, U. S. Department of Energy under contract No. DE-AC03-76SF00098.

TABLE OF CONTENTS

THE OBSERVATION OF THE HABIT PLANE SHIFT AND THE MORPHOLOGY OF α" NITRIDE ($Fe_{16}N_2$) PRECIPITATE IN α-Fe

Yih-Cheng Shih

Master of Science

Materials Science and
Mining Engineering

Chairman of Committee

ABSTRACT

The habit plane shift phenomenon of α" nitride ($Fe_{16}N_2$) precipitate in α-Fe is discovered by TEM observation. The habit plane of α" precipitate shifts from {100} toward {102}. The angular shift increases as the precipitate grows. Also, the angular shift increases as the aspect ratio of α" particle increased. This relation has been predicted by considering the finite thickness effect on Khachaturyan's elastic theory. The crystal structure of the habit shifted precipitate is found to be distorted from a tetragonal structure, the structure of the initial α" precipitate.

The real morphology of α" precipitate at the early stage is revealed as a rosette pattern on {001} habit plane. The branches of the rosette point in <100> and <110> directions. The possible reasons for the rosette morphology are discussed. The aspect ratio data of α" precipitates are obtained by TEM direct measurement. Due to the limitation of resolution, no precise conclusion can be made on the relationship between aspect ratio and particle size during coarsening.

I. INTRODUCTION

The free energy change during phase transformation involves three terms, which are volume free energy change ΔF_v , surface energy change ΔF_s , and elastic strain energy change ΔF_e .

$$\Delta F_{tot} = -\Delta F_v + \Delta F_s + \Delta F_e \ .$$

But only two of them, surface energy and elastic strain energy, are concerned with the shape and the habit plane of a coherent precipitate particle. The shape of a coherent nucleus is generally determined by the relative values of the elastic constant, the magnitude of lattice mismatch and the anisotropy of surface energy (1). If the lattice mismatch between precipitates and the matrix is very small, the elastic strain energy is less important than the surface energy. Then, the criterion of minimum surface would dominate the shape of precipitates. Spherical precipitates would be formed in this case. On the contrary, if the surface energy is negligible compared with the elastic strain energy of coherent precipitates, the elastic strain energy would strongly influence the shape of precipitates. The precipitates of various shapes, such as disc, needle, ellipsoid etc., could be formed.

The habit plane of the plate precipitates reflects the need to accommodate the elastic strain induced by its crystallographic mismatch with the parent matrix. One phenomenological theory of the prediction of the habit plane deals with a set of geometric relationships which determines a habit and internal structure of the precipitate plate, leading to a strain-free match across the interface in the habit plane (2). Another approach to the prediction of the preferred habit plane is to minimize

the elastic strain energy, as a function of the normal direction of the habit plane of the precipitates (3).

The elastic strain energy is not only important in determining the shape and the preferred habit plane of the precipitates, but also in materials strengthening. The elastic interaction between the dislocations and the precipitates is the essential obstacle to dislocation propagation.

J. D. Eshelby (4) first calculated the elastic strain energy of a coherent ellipsoid shaped particle in a continuous isotropic medium in 1957. Lee, Barnett and Aaronson (5) developed Eshelby's work to account for anisotropic media. In 1967, Arman, G. Khachaturyan (6) developed a formula to calculate the elastic strain energy of arbitrary shaped inclusion in anisotropic medium by using a Fourier transformation technique. The same elastic modulus of the inclusion and the parent matrix was assumed in the calculation.

Khachaturyan's formulation was applied successfully to the computer simulation of the martensite transformation and tweed formation (7,8). The preferred habit plane of plate precipitates in a cubic matrix has been predicted by minimizing the elastic strain energy as given by Khachaturyan linear elastic formula (3). The preferred habit plane of the finite thickness precipitate was also numerically calculated (9). In addition, the elastic strain energy of the disc, lens and ellipsoid-shaped particle was simplified as a function of any two of the dimensional parameters of the precipitated particles that the computer calculated from this formula (10).

The prediction of the preferred habit plane is consistent with experimental evidence in the case of G. P. zones in Al-Cu and Cu-Au, Fe_4C precipitates in α-Fe and β-$VH_{0.45}$ precipitates in vanadium (3). α''

nitride ($Fe_{16}N_2$) precipitates (11) in α-Fe have similar tetragonal transformations with Fe_4C in α-Fe . However, the observed habit plane of α" ($Fe_{16}N_2$) precipitates in α-Fe is {100}[12-14], rather than {102}[15,16], the habit plane of Fe_4C in α-Fe either from the experimental result or from the theoretical predictions (3,9). This difference could be explained by considering the finite thickness effect on α" nitride precipitate (9).

By theoretical calculation (9), the preferred habit plane of α" precipitate is (100) when $K < 11.34$ and shifts toward (102) plane when $K > 11.34$. (Where the aspect ratio $K \equiv 2R/Z$, R being the radius of the disc, and Z the thickness.) In the present work, the habit plane shift phenomenon was observed. The extent of angular shift from (100) increases as aspect ratio increases.

The elastic strain energy of a thin plate precipitate can be a simple function of the aspect ratio, when the dislocation loop model was considered for a thin plate precipitate (17). During the coarsening of the plate precipitate, the aspect ratio of the plate should maintain a certain relation with the diameter, by minimizing the summation of the elastic strain energy and the surface energy in a equilibrium shaped particle. Three sets of aspect ratio data (12,18,19) satisfy this relation individually, but the relation breaks down when all the data are considered together (10). Therefore, it is suggested that direct measurements of the aspect ratio of α" precipitates should be made from TEM observations, to test the relation again. Unfortunately, the thickness of the coherent α" precipitates is below that which could be measured directly and accurately in the TEM.

An interesting rosette pattern morphology of α'' precipitates on {100} planes was revealed in this work; reasons for this particular morphology will be discussed.

II. THEORETICAL REVIEW

A. The Elastic Energy of a Coherent Precipitate

Khachaturyan's expression for the elastic energy of a coherent inclusion, can be obtained either from the macroscopic elastic theory (6) or the continuum limit of the microscopic linear elastic theory for a discrete lattice (20). Both derivatives have been discussed in details by Khachaturyan himself, and other authors (7,9).

Only the essential concepts and the simple results of the macroscopic derivative are briefly described here. Khachaturyan used Eshelby's imaginary cycle [4] of a precipitate formation, to calculate the total elastic strain energy of a coherent precipitate in the parent matrix. The Eshelby Cycle is shown in Fig. 1, and described below:

(1) An inclusion to be transformed is removed from the parent matrix without changing its shape or size. (2) This inclusion is transformed to a new phase with stress-free strain. (3) Surface tractions are applied to restore the inclusion to its original shape. The strain here is the reverse of that during the transformation, i.e., $-\varepsilon^0_{ij}$. The final stress is σ^0_{ij} or $\lambda_{ijlm}\varepsilon^0_{lm}$. So, the energy required in this step is

$$F_3 = \frac{1}{2}\,\sigma^0_{ij}\varepsilon^0_{ij}V = \frac{1}{2}\,\lambda_{ijlm}\varepsilon^0_{lm}\varepsilon^0_{ij}V \ ,$$

where V is the volume of the inclusion. (4) The transformed inclusion is put back into the hole left in the matrix. (5) Then, the inclusion and the matrix are allowed to relax together into their equilibrium configuration. The relaxation energy of the matrix and the inclusion are involved in this step,

$$F_5 = F_5(\text{matrix}) + F_5(\text{inclusion})$$

$$= \int_{\text{matrix}} \frac{1}{2} \lambda^{(m)}_{ijlm} \varepsilon_{ij} \varepsilon_{lm} dv + \int_{\text{inclusion}} \left[-\sigma^0_{ij} \theta(r) \varepsilon_{ij} + \frac{1}{2} \lambda^{(in)}_{ijlm} \varepsilon_{ij} \varepsilon_{lm} \right] dv ,$$

under the assumption of the same elastic modulus in both phases,

$$F_5 = \int_V \left[-\sigma^0_{ij} \theta(r) \varepsilon_{ij} + \frac{1}{2} \lambda_{ijlm} \varepsilon_{ij} \varepsilon_{lm} \right] dv ,$$

where λ_{ijlm} is the fourth rank tensor of elastic modulus, is the elastic strain, and $\theta(r)$ is a form function, which is equal to one inside the inclusion and zero otherwise.

Obviously, steps (1), (2) and (4) involve no energy change. Therefore, the total elastic strain energy of a cohernt precipitate is: $F_E = \frac{1}{2} \lambda_{ijlm} \varepsilon^0_{ij} \varepsilon^0_{lm} V - \int_V \left[-\sigma_{ij} \theta(r) \varepsilon_{ij} + \frac{1}{2} \lambda_{ijlm} \varepsilon_{ij} \varepsilon_{lm} \right] dv$. By using Fourier transformation on the integration term,

$$F_E = \frac{1}{2} \lambda_{ijlm} \varepsilon^0_{ij} \varepsilon^0_{lm} V - \frac{1}{2} \iiint_{-\infty}^{\infty} B(e) |\theta(k)|^2 \frac{d^3k}{(2\pi)^3}$$

where $e = \frac{K}{|K|}$ is a unit vector in the K direction $B(e) = e_i \sigma^0_{ij} \Omega_{ij} \sigma^0_{lk} e_l$ is a function of direction depending on the elastic moduli of the materials and on transformation strain. $\Omega_{ij} = |K|^2 G_{ij}$, $G_{ij} = D^{-1}_{ij}$ is Green's function, and $\theta(k) = \iiint_{-\infty}^{\infty} e^{ik \cdot r} \theta(r) d^3r$ is a shape factor which is the Fourier transform of the form function $\theta(r)$.

B. The Preferred Habit of a Plate Tetragonal Inclusion in a Cubic Matrix

The preferred habit plane of a coherent precipitate must reflect the need to accommodate the elastic strain induced by its crystallographic mismatch with the parent matrix. If the mismatch is large, this elastic strain would dominate the surface energy effects in determining the preferred habit. In this case, the preferred habit can be predicted by minimizing the elastic strain energy of a coherent particle as a function of its crystallographic habit.

$$\left.\frac{\partial F_E}{\partial e}\right|_{e=n} = 0 \qquad \left.\frac{\partial^2 F_E}{\partial e^2}\right|_{e=n} > 0 \ ,$$

where e is the unit vector of K direction, n is the normal of the habit plane of the plate precipitate.

(a) Zero - thickness Approximation

If the inclusion is considered arbitrarily thin, $\theta(k)$, the shape factor, becomes a Dirac δ-function, i.e., the $\theta(k)$ has value only when e is close to n direction.

$$F_E = \frac{1}{2}\lambda_{ijlm}\varepsilon^0_{ij}\varepsilon^0_{lm}V - \frac{1}{2}\int B(n)|\theta(k)|^2\frac{d^3k}{(2\pi)^3}$$

$$= F_0^E V - \frac{1}{2}B(n)\int|\theta(k)|^2\frac{d^3k}{(2\pi)^3}$$

$$= F_0^E V - \frac{1}{2}B(n)V \ .$$

By using eqn. $\frac{\partial B(n)}{\partial n} = 0$, $\frac{\partial^2 B(n)}{\partial n^2} > 0$ and symmetric geometric relations in cubic matrix and tetragonal inclusion, several analytic results can be obtained [3].

1. The preferred habit plane of the tetragonal inclusion is a plane of the type (hol) or (okl), if the anisotropy factor $\Delta < 0$ and is a plane of the type (hhl), if $\Delta > 0$.

2. When $\Delta < 0$, the preferred habit plane has Miller indices (hol) (or (okl)) corresponding to the triplet (n_1, n_2, n_3) , where n_3 , the component of the normal vector along the tetragonal axis, satisfies the relation:

$$n_3^2 = \begin{cases} 1 + \Lambda/(\mu\eta) & \text{where} \quad -\infty \leq \eta \leq -\Lambda/\mu \\ 0 & \quad -\Lambda/\mu < \eta \leq 0 \\ 1 & \quad 0 < \eta < \infty \end{cases} ,$$

where $\eta = (\varepsilon_{33} - \varepsilon_{11})/\varepsilon_{11}$, is the tetragonality of the transformation strain.

$\Delta = C_1 - C_2 - 2$ is the anisotropy factor.

$$\Lambda = C_1 + 2C_2 ,$$

$$\mu = C_1 + C_2 ,$$

where $C_1 = C_{11}/C_{44}$, $C_2 = C_{12}/C_{44}$, are the elastic coefficients of the matrix

$$n_1^2 + n_2^2 + n_3^2 = 1 .$$

3. When $\Delta > 0$, the preferred habit plane has Miller indices (hhl) derived from the triplet (n_1,n_2,n_3) , where n_3 , the component of the normal vector along the tetragonal axis, satisfies the relation:

$$n_3^2 = \begin{cases} -\dfrac{(\Delta + 4)\Lambda - (\Delta\Lambda + 4\mu)\eta}{\Delta\Lambda - (\Delta\Lambda + 4\mu)\eta} & , \quad -\infty < \eta < \eta_1^+ \\ 0 & , \quad \eta_1^+ < \eta < \eta_2^+ \\ \dfrac{\Delta\Lambda + (\Delta\Lambda + 4C_1)}{\Delta\Lambda(3 + \eta)} & , \quad \eta_2^+ < \eta < \eta_3^+ \\ 1 & , \quad \eta_3^+ < \eta < \infty \end{cases} ,$$

where

$$\eta_1^+ = \frac{-(\Delta + 4)\Lambda}{\Delta\Lambda + 4\mu} \quad , \quad \eta_2^+ = \frac{-\Delta\Lambda}{(\Delta\Lambda + 4C_1)} \quad ,$$

$$\eta_3^+ = \frac{\Delta\Lambda}{2C_1} \, .$$

For example:

(i) The early stage carbide precipitate formed from martensite, on aging near room temperature, is believed to have composition Fe_4C and is found in the form of a thin plate with a (102) habit [15,16]. The habit plane predicted from above equations is (0.382 , 0 , 0.924) by using $\eta = -10$, and $\Delta < 0$. The prediction gives an angle $\theta = 22°$ between the habit normal and the tetragonal axis. It is within 5° difference with the observed habit (102), $\theta = 26.6°$

(ii) $\beta - VH_{0.45}$ precipitate in vanadium has an unusual habit of (227) [2]. The predicted habit normal for $\Delta > 0$, and $\eta = -10$ is at an angle $\theta = 22.18°$, from the tetragonality axis in the (110) plane, com-

pared with the angle between (227) and (110), $\theta = 22°$.

(b) Finite thickness calculation [9]

When some precipitate of an initially thick plate, like $Fe_{16}N_2$ is considered for the habit prediction, the zero-thickness approximation in elastic energy calculation can not be used anymore. The Fourier transform of the shape function $\theta(r)$ is given as:

$$\theta(k) = 2 \cdot V \frac{\sin\left(|K| \cdot \cos\alpha \cdot \frac{z_0}{2}\right)}{|K| \cdot \cos\alpha \cdot \frac{z_0}{2}} \frac{J_1(|K| \cdot \sin\alpha \cdot R_0)}{|K| \cdot \sin\alpha \cdot R_0}$$

and $B(e)$ can be expressed as a function of α and β angles, which were indicated in Fig. 2. So the elastic strain energy is

$$F_E = F_0 - \frac{1}{2}\int_0^{\pi}\int_0^{2\pi} \frac{1}{(2\pi)^3} B(\alpha \cdot \beta) f(\alpha) \sin\alpha d\alpha d\beta ,$$

where

$$f(\alpha) \equiv \int_0^{\infty} |\theta(k)|^2 k^2 dk .$$

By minimizing the elastic strain energy as a function of the habit normal direction, the habit of the tetragonal precipitate in cubic matrix can be predicted. It is impossible to integrate the above equation analytically, and only a numerical solution can be obtained by computer calculation. For instance, the habit plane of $\alpha''(Fe_{16}N_2)$ precipitate in α-Fe has been calculated as a function of α , the angle between the habit normal with the tetragonality axis, and aspect ratio K , $\frac{2R}{Z}$. (Where R is

the radius of the disc, and Z the thickness.) The result is tabulated in Table I. The habit plane predicted from theory remains on (100) when $K < 11.34$; and it shifts toward (102), when $K > 11.34$. The angular shift from (100) is 22.5°, when K approaches infinite. The angular shift increases as aspect ratio increases. The relation was diagrammed in Fig. 3.

In the literature, many authors [11,12-14] report that the habit plane of α'' ($Fe_{16}N_2$) precipitate is {100}. No habit plane shift phenomenon was observed. It is an interesting and challenging topic to find out exactly whether the habit of α'' precipitate would shift away from {100} as the aspect ratio increases. Otherwise, it is also worthy to get the reasons explaining why the prediction does not work in this case.

C. The Change of Aspect Ratio on Coarsening

In 1973, Khachaturyan [17] presented a calculation of the elastic strain energy of a thin plate precipitate, using the assumption of very large aspect ratio K . The elastic energy of the thin plate was considered to be associated with the edge, as if it were bounded by an edge discolation loop. In this model, one needs only to deal with the x-y plane, orienting the z-axis normal to the plate. The elastic strain energy of the plate can be expressed in a very simple formula:

$$F_E = \frac{\beta V}{\pi} \frac{\ln K}{K} ,$$

where β is constant related with elastic modulus, V is the volume of the plate, and K is the aspect ratio.

If the plate precipitate is in equilibrium shape during coarsening, the combination of the elastic strain energy and surface energy of the

precipitate should be in a minimum point. The surface energy of the plate is

$$F_s = \gamma A = \gamma \cdot (CV^{2/3}K^{2/3}) \ ,$$

where γ is the interface energy per unit area, A is the surface area of the particle, C is a constant of shape.

$$F_T = F_E + F_s$$

$$= \frac{\beta V}{\pi} \frac{\ln K}{K} + C\gamma V^{2/3}K^{2/3}$$

$$\left(\frac{\partial F_T}{\partial K}\right)_V = \frac{\beta V}{\pi} \frac{\ln K - 1}{K^2} + \frac{2}{3} C\gamma V^{2/3}K^{-1/3} = 0$$

$$\gamma = \frac{3}{4\pi} \beta \frac{D(\ln K - 1)}{K^2} \ ,$$

where D is the diameter of the disc. So the unit surface energy can be calculated, if the loop model is appropriate for the thin plate precipitate and the precipitate is in an equilibrium shape.

The unit surface energy is considered a constant before the precipitate becomes semicoherent. Then

$$\frac{D(\ln K - 1)}{K^2} = \text{constant} \ .$$

If the $\frac{K}{\sqrt{\ln K - 1}}$ value versus D value is plotted, the figure is a straight line. This relation can be used as a test of the usefulness of the loop model.

Three sets [12,18,19] of aspect ratio and diameter data of α'' precipitates in α-Fe satisfy this relation individually, but the relation breaks down when all the data are considered together. The data sets are

listed in Table II, and shown in Fig. 4. Keh and Wriedt's data [12] were obtained by indirect measurement. They used an internal friction method to estimate the precipitation percentage, and measured the average diameter of the precipitate, then calculated the thickness. Abiko and Imai's data were also obtained by indirect measurement using an electrical resistance method [19]. Wagner and Brenner [18] used Field Ion Microscope to measure the aspect ratio of α" precipitate, which is $(Fe, Mo)_{16}N_2$ in composition, aged at 600°C from Fe-3 at % Mo nitride alloy.

Apparently, the break down of the relation is possibly caused by the different and indirect measuring methods of the aspect ratio, in the three sets of data. In addition, the difference of the composition of α" precipitate and aging temperature, in these three sets are also the possible reasons of failure. Hence, a systematic and direct measurement of the aspect ratio of the coherent α" precipitate by TEM is carried out in this experiment, to rigorously test the theory.

III. EXPERIMENTAL PROCEDURE

A. Materials Preparation and Heat Treatment

The alloy needed to precipitate α" ($Fe_{16}N_2$) nitride metastable phase is constituted by iron and nitrogen only. Therefore, the Fe-N alloy was prepared as pure as possible, in order to avoid unexpected precipitates, by other impurity atoms. The concentration of nitrogen was designed as low as 0.01 wt% (~0.04%), so that the nitrogen could constitute 0.35% volume of α" particles in α-Fe matrix. The reason for low concentration of nitrogen, is to avoid strong elastic interactions, among densely distributed α" precipitates.

Iron nitride (Fe_2N) powder and pure iron chips (99.99%) were arc-melted and mixed together under a low pressure of argon atmosphere to form 100 gm ingots. These ingots, sealed in quartz tube, were homogenized at 1200°C for 24 hrs.then hot-rolled at 800°C to 40 mil (1 mm) thickness and cut to the size of 1" × 2". Solution treatment was carried out at 750°C for 3 hrs. An ice water quench was used after each heat treatment. One small piece of each ingot was sent for chemical analysis. The nitrogen content was 0.011 wt% with carbon lower than 0.004 wt%. S and P were also found to be lower than 0.005 wt%.

The specimens were aged in an Al_2O_3 powder fluidized bath or oil bath, for several periods of time to obtain different sizes of precipitates. The aging temperature varied from room temperature to 150°C.

B. Transmission Electron Microscope

1. Preparation of TEM Specimen

(a) Thinning Process

Mechanical thinning was avoided since it introduces too many disloca-

tions into the material of the present work. Chemical thinning was applied only in the process of producing a 2-3 mil thickness foil. The chemical solution was 10 ml. HF (48%) + 190 ml. H_2O_2 (30%). Magnetic stirring and cold trapping with liquid nitrogen were provided in chemical thinning to prevent preferential etching and extra heating.

(b) The foil was punched to 2.3 mm diameter discs. The stigmatism induced by ferromagnetic specimen is 40% lower by using 2.3 mm diameter discs rather than the normal 3 mm disc. Although the heating during spark cutting is minimal, it still influenced the α'' nitride precipitation seriously. Therefore, we used punch, instead of spark cutting, to prevent extra heating during spark cutting.

(c) Jet Polishing

The disc was jet polished in a solution of (75 gm CrO_3 + 400 ml. CH_3COOH + 20 ml. H_2O) at an optimum voltage of 30-35 volt and an optimum current of 18-20 mA. The brightness of the penetrating light in solution must be enough to be detected, when just a very small hole is formed. It depends on the above procedure, whether the specimen foil is good or not. To prevent oxidization in the surface of specimens, careful cleaning of specimen by ethelene alcohol 200 proof is followed, as soon as the disc is taken out from the solution.

2. TEM Observation

(a) The thickness measurement can only be carried out when the precipitate is edge-on. Therefore, the specimens had to be tilted to make the precipitates edge-on first. The accuracy of the tilting was deter-

mined by reference to Kikuchi maps. Then, the weak beam dark field and dark field taken from the diffraction spot of the precipitate, were applied to measure the thickness of the precipitate as accurately as possible. Because the best resolution obtainable in the image mode in TEM, is 10-15 Åm we have little confidence in the measurement of the precipitate thicknesses less than 20 Å.

(b) The determination of the habit plane of the precipitates had to be worked out by trace analysis [20]. For example, if the habit plane is {100}, three variants of the inclined precipitates can be seen in the [111] pole, and two edge-on and one lie-on variants of the precipitates in the [100] zone axis. To make sure that the precipitate is edge-on, the specimen needs to be tilted away from edge-on direction and compare the thickness of the images taken in different directions. In Fig. 5, it is supposed that the precipitate is edge-on in the {102} pole, i.e., at A point in the Kikuchi map. Then, the observed grain was tilted several degrees away from A to B and C points. Points B and C are symmetrical to A . If the image width of the precipitate at A is smallest, compared with that at B and C , the precipitate is exactly edge-on at A zone axis. When the shifted and unshifted habit planes are both edge-on, the shifted angle of the habit plane can be measured.

(c) The Philips 301 and the JEOL 100C TEM were both used in this experiment, and operated at 100 Kev. The double tilting stage of the Philips 301 has a maximum tilt angle of $\pm 45°$ in the X axis and $\pm 25°$ in the Y axis. The maximum tilt angle of the JEOL 100C's double tilting holder is $\pm 60°$ in both axes. It is rather difficult to tilt the specimen from the [111] pole to the [100] pole, because the angle between these

two poles is 54°44'. Owing to the JEOL 100C's high angle tilting function, the JEOL 100C was used to solved the above problem.

IV. EXPERIMENTAL RESULTS

A. The Morphology of α" Precipitate in α-Fe .

The shape of α" nitride precipitate was reported as a disc or plate by many authors (12,13,18,19,22). A lamella shape of α" precipitates was also observed by Garwood and Thomas (14), as the deviation of the plate owing to the high volume fraction of the precipitate (~50%). Moreover, Keh and Wriedt (12) mentioned that the peculiar contrast effects exhibited by the α" particles suggested that they were circular discs of nonuniform thickness. The equilibrium shape of a precipitate is determined by the combination of the effects of the elastic energy and surface energy. The discovery of the real morphology of a precipitate can clarify the roles of the elastic energy and surface energy in contributing to the determination of the shape of the precipitate.

The morphology of α" nitride precipitates of the Fe-0.011 wt.%N alloy, aged at 100°C for 10 min. and at room temperature for two months, appears as a flower pattern with discontinuities in several directions (Fig. 6). This figure was taken in [111] beam direction. The average diameter of the precipitates is about 1000 Å.

When the precipitate was observed near the [319] zone axis, which is 19° away from [001], a rosette pattern of the α" precipitate on the habit plane of (001) was revealed (Fig. 7). The eight branches of the rosette pattern point in <100> and <110> directions.

These particles were then examined under different foil orientations to establish a maximum variety of local diffraction conditions. In this way, all possible "disappearance" effects (where $\underset{\sim}{g} \cdot \underset{\sim}{R} = 0$, $\underset{\sim}{g}$ being the diffraction vector: $\underset{\sim}{R}$, the displacement vector associated with any segment of the particle) were observed. These contrast experiments verified

the shape of the particles. They are truly rosettes and not affected by imagining artefacts.

In the later stage of the α" precipitate, aged at 150°C for 100 min., the rosette still existed (Figs. 8a,b). The branches of the precipitate merged together, but the small portions on the edge of the precipitate remained unprecipitated along the difficult growth direction <102>. Figures 8c and 8d show that <112> are the projected directions of <102> in [111] zone axis. The fringes in Fig. 8c are Moire fringes, which are excited by the interference of the different interplanar spacing in the precipitate and matrix for the parallel crystallographic planes.

B. The Habit Plane Shift Phenomenon of α" Precipitate

No one has reported the habit plane shift of α" precipitates in the literature previously. However, in this experiment the habit plane shift is observed either at an early stage or at a later stage of the α" precipitates.

The precipitate in Fig. 7 is a nearly edge-on precipitate of the (100) habit plane. A small branch on the right hand side of A precipitate is believed to be the habit-shifted precipitate at an early stage. The shifted angle from (100) is about 12°. Figure 9, as a DF image taken from the combination of 200 matrix spot and 400 precipitate spot in [001] beam direction, shows the shifted habit plane. The shifted angles vary from 13° to 15°.

In the later stages of α" precipitation, the shifted angle from the (100) habit increases to 19°, as in Fig. 10. Figure 10a is a BF image taken near the [111] zone axis. Figure 10b is a DF image taken from $0\bar{1}1$ matrix diffraction spot and $0\bar{2}2$ precipitate spot in [111] beam

direction. Both images show that the inclined precipitate consisted of eight pieces that connect with each other. The specimen was tilted to make the precipitate edge-on as in Fig. 10d, BF, and in Fig. 10e, DF, taken from $\bar{2}00$ matrix spot in [012] zone axis. The first upper piece of the precipitate has a habit which remains on (100). The habit plane of the lower pieces shifts away from (100) about 19°. The observed shifted angle increases as the precipitate grows, or increases as the aspect ratio increases. The data are tabulated in Table III and are diagrammed in Fig. 3.

A continuously curved precipitate was also observed in Fig. 11a, which is a BF image taken in a symmetrical orientation very close to a [001] pole. The trace of [100] direction is marked to compare with the edge-on and curved precipitate in order to show that the shifted angle is 18.5°. The DF image from 020 precipitate spot is taken in Fig. 11b. The thickness of the precipitate is 136 Å at the central part and 20 Å at the end. With regard to the thickness distribution, the two smaller pieces at the right hand side should belong to this precipitate.

The electron diffraction pattern of Fig. 11a shows that the 020p is splitting into two separate streaks (Fig. 11c). One is exactly along the [020m] direction; the other one, which is believed to be from the shifted part of the precipitate, is about 1° deviation from the [020m] direction. The tetragonal axis, which is [020p], is about 8.2% longer than $2a_o$ of the α-Fe matrix. The separation between the two streaks in the $\bar{2}00p$ shows that the lattice parameter in the [200] direction of the shifted part of the precipitate is 1.6% longer than that of the unshifted part. Therefore, the crystal structure of the shifted precipitate is distorted from the tetragonal structure.

The habit plane shift phenomenon was also checked in the inclined directions. The inclined precipitate with the habit of {100} is indicated as A , and the habit plane shifted part is marked as B in Fig. 12. Some of the α" precipitates still remain on {100} habit as in Fig. 12a. The others shift their habit plane from {100} toward {102} (Fig. 12b-f). Figure 12c is the DF image of Fig. 12b, which is taken in the [389] beam direction. The Weak Beam Dark Field is also taken here to observe details. The specimen is tilted to [011] zone axis (Fig. 12e) and [012] zone axis (Fig. 12f) to check the trace of the habit-plane shifted precipitates. The zone axes in which in which the pictures were taken are marked at the upper left corner of the pictures. The zone axis directions can be referred to in the schematic Kikuchi map, Fig. 5.

C. The Aspect Ratio Data

The measurement of the thickness of α" precipitates must be carried out at the precipitate edge-on direction. Because the habit plane of the initial stage precipitate is {100}, at least one variant of the {100} habit is edge-on in the <200> Kikuchi path. Only the Weak Beam Dark Field and Dark Field from the diffraction spots of the precipitate were taken to obtain better resolution in the thickness measurement. The best resolution obtainable is 10-15 Å. Hence, no thickness data less than 20 Å was recorded. The thickness of α" precipitates measured range from 20 Å to 136 Å. The diameter of the precipitates range from 1700 Å to 1.8 μm. All the data are listed in Table II and diagrammed in Fig. 4. The aspect ratio data which was measured directly using TEM are higher than that of the indirect measurement by Keh and Wreidt or Ahiko and Imai when the same diameter of α" precipitate is considered.

Due to the limitation of the TEM resolution, no directly measured aspect ratio data of α'' precipitates that are less than 1500 Å in diameter was obtained. The tetragonality of α'' precipitate is 10% dilatation as reported (11) or 8.2% as in this experiment. This large mismatch could make the α'' precipitate, which larger than 50 Å in thickness or 5000 Å in diameter, lose the coherence with the matrix. Therefore, no conclusion about the aspect ratio relation with the size of the coarsening precipitate can be made.

V. DISCUSSION.

A. The Possible Reasons for the Rosette Morphology

The morphology of α" precipitates in the early stage are revealed as a rosette pattern on the habit of {100} with eight branches toward the <100> and <110> directions. The possible sources that make α" particles precipitate in this particular morphology are generalized in three respects:

(1) Both the anisotropic elastic constrants and the lattice distortion of the precipitate and the matrix can induce anistropic elastic strain in the <100> habit plane. The elastic strain energy of the α" precipitate should be calculated using the Khachaturyan formula in the shapes of rosette pattern and circular disc. If the elastic energy of a rosette pattern appears lower than that of a circular disc, obviously the rosette morphology is dominated by the anisotropic elastic strain effects.

(2) The elastic interaction from the neighboring precipitates can also influence the morphology of the α" precipitate. In 1969, Khachaturyan and Shatalov (23) calculated the elastic interaction energy between two inclusions. If the inclusions are tetragonal crystal geometry transformation, the extrema of the elastic interaction potential, with perpendicular tetragonality, lie along the symmetrical directions <100> and <110> on a (001) cross section. The elastic interaction could be important to the early stage precipitates that are in short distance with each other. If the self anisotropic elastic energy cannot explain the rosette morphology, the interaction energy should be considered.

(3) The third possibility of explaining the rosette morphology is the anisotropic surface energy. The surface energy here is only defined

as a chemical energy on the interface of a precipitate and the matrix. The surface energy has a minor effect compared with the elastic energy in the case of α" nitride precipitate. However, if the elastic energy is isotropic on the (100) plane, the anisotropic surface energy will be the main influence upon the morphology of α" precipitates.

B. Habit Plane Shift Phenomenon

(1) The process of a habit plane shift. Figure 10 shows that the habit-shifted part of the precipitate consisted of seven small pieces. Although the connection line of these edge-on pieces deviates from the (100) habit plane by about 19° (Fig. 10d-e), the small pieces individually change their habits at lower degrees than the common habit does. The phenomenon may strongly hint that the process of the habit plane shift involves a transition state of small pieces shift in order to detour the strong resistance from large angle movement. Eventually the small pieces would grow into one piece and the habit plane is continuously curved, as in Fig. 11.

(2) The α" nitride precipitate is considered to be the nitrogen diffusion-controlled growth (19). Hence, the α" precipitate grows very fast. For instance, the average diameter of an α" precipitate aged at 100°C for 10 min. is about 1000 Å, and the average diameter of an α" precipitate aged at 150°C for 100 min. is 1.5 μm. It is very possible that the α" precipitate is in quasi-equilibrium shape after being aged at a higher temperature for a short period of time. Also, the habit plane would remain on the initial habit (100) even when the aspect ratio is larger than 11.34, as in Fig. 12a. An interesting temperature effect can be found by comparing the sizes of the unshifted parts of α" precipitates.

The average diameter of the unshifted part of an α" precipitate aged at 100°C is around 1000-1500 Å (Figs. 7 and 9) while in Figs. 10, 12 and 13 the average diameter of the unshifted part aged at 150°C is 3000-5000 Å.

(3) The electron diffraction evidence shows that the crystal structure of the habit-shifted precipitate is distorted from tetragonal structure. One author (24) claimed that the habit plane shift was caused by the crystal structure change of the precipitate. Therefore, the elastic distortion or real crystal change should be clarified in this case. Convergent Beam Diffraction can be applied later on to investigate the crystal structure of the unshifted precipitate and the habit-shifted precipitates at different shifted angles. The electron diffraction of the shifted precipitate in a stress-free condition should be checked by using a replica extraction technique in TEM. So far, the crystal structure of the habit-shifted precipitate is believed to be elastically distorted by the internal strain in the precipitate, from consideration of Khachaturyan's elastic theory.

(4) Because the aspect ratio is hard to obtain by direct measurement, and the habit shift phenomenon was not noticed at the beginning of this experiment, only two data points in Fig. 3 show that the shifted angle increases as the aspect ratio increases. In addition, more data is needed to show that the shifted angle increases as the precipitate grows as in Table III. In Table II and Fig. 4, the aspect ratio increases as the precipitate grows. The relation implies that the shifted angle increases as the aspect ratio increases. Additional aspect ratio data, as well as the habit-shifted angles, are needed to perfect this argument.

C. The Coherence of α" Precipitates

The application of Khachaturyan's elastic theory is only for coherent particles. It is hard to define the coherence of a precipitate from various statements in the literature. It is also difficult to determine the coherence of a precipitate by experiment. The thickness increase of the α" precipitate makes the precipitate become semi-coherent, then incoherent with the matrix, due to the misfit at the interface being too large to be accommodated. The thickness of α" precipitates becomes a lens distribution when the precipitate is large. For example the thickness is 136 Å at the central part and 20 Å at the ends of the precipitate (Fig. 11). In this way the large precipitate may keep its coherence at the edge of the plate. Also, the lens shape can distribute the large misfit along the habit plane into several steps, hence the coherence may be kept at each step. Unless the lattice image of the α" precipitate can be taken, the maximum size of an α" coherent precipitate is uncertain. As soon as the precipitate becomes semicoherent, the elastic energy of the precipitate will be reduced a great deal by introducing interface defects or disorder zone. Then the elastic energy for the semicoherent and incoherent precipitate is too complex to be estimated.

The large precipitates observed in Figs. 10, 11 and 12 might have lost their coherency with the matrix. However, the theoretical prediction of the habit plane shift only deals with coherent precipitates. Therefore, the difference about the habit-shifted angle between the theoretical calculation and the experimental result can be expected, as in Fig. 3. In this case, the surface energy effect has a more important influence on the determination of the habit plane, and should be considered in the interpretation of the habit plane phenomenon.

D. The Aspect Ratio of Small Precipitates

If the thickness of small precipitates are less than 20 Å, the lattice images should be taken to obtain enough aspect ratio data of coherent precipitates to test the aspect ratio relation. The aspect ratio data of large precipitates must be taken carefully because the length of the edge-on precipitate is less than the real diameter when the large precipitate is cut in the non-central part by the TEM foil.

VI. CONCLUSION

1. The habit plane of α" precipitate shifts from {100} toward {102} when the precipitate grows. The shifted angle increases as the size of the precipitate increases. Also, the shifted angle increases as the aspect ratio increases, as predicted in Khachaturyan's elastic theory.

2. The crystal structure of the precipitate of which the habit plane shifts 18.5° away from {100} is distorted from a tetragonal structure. The tetragonality axis is 8.2% longer than $2a_o$ of the α-Fe matrix. The other axis is 1.6% longer than $2a_o$ of the α-Fe matrix, and the angle between these two axes is 91°.

3. The morphology of an early stage precipitate, which has an average diameter of 1000 Å, is a rosette pattern lying on the {100} habit plane. The eight branches of the rosette morphology point in the <100> and <110> directions. The difficult growth directions are <102>.

REFERENCES

1. J. W. Martin, "Precipitation Hardening", Part I. Pergamon Press (1968).

2. J. S. Bowles, B. C. Muddle, and C. M. Wayman, Acta Metall. 25, 513 (1977).

3. S. H. Wen, E. Kostlan, M. Hong, A. G. Khachaturyan, and J. W. Morris, Jr., Acta Metall. 29, 1247 (1981).

4. J. D. Eshelby, Proc. Roy. Soc. A241, 376 (1957).

5. J. K. Lee, D. M. Barnett, and H. I. Aaronson, Met. Trans., 8A 963 (1977).

6. A. G. Khachaturyan, Sov. Phys. Solid State, 8, 2163 (1967).

7. S. Wen (Chen), Ph.D. Thesis, Dept. of Materials Science and Mineral Engineering, University of California, Berkeley, (1979).

8. S. Wen, A. G. Khachaturyan, and J. W. Morris, Jr., Met. Trans, 12A, 581 (1981).

9. M. Hong, M.S. Thesis, Dept. of Materials Science and Mineral Engineering, University of California, Berkeley, (1978).

10. D. E. Wedge, M.S. Thesis, Dept. of Materials Science and Mineral Engineering, University of California, Berkeley, (1980).

11. K. H. Jack, Proc. Roy. Soc., A208, 216 (1951).

12. A. S. Keh and H. A. Wriedt, Trans. Met. Soc. AIME, 224, 560 (1962).

13. K. F. Hale and D. McLean, J. Iron & Steel Inst., 201, 337 (1963).

14. R. D. Garwood and G. Thomas, Met. Trans. 4, 225 (1973).

15. S. Nagakura, K. Shiraishi, and Y. Hirotsu, Trans. Japan Inst. Metals 16, 601 (1975).

16. V. I. Izotov and L. M. Uterskiy, Phys. Metall. 25, 86 (1968).

17. A. G. Khachaturyan and V. N. Hairapetyan, Phys. Stat. Sol. B57, 801 (1973).

18. R. Wagner and S. S. Brenner, Acta Metall. 26, 197 (1978).

19. K. Ahiko and Y. Imai, Trans. Japan Inst. Metals, 18, 113 (1977).

20. A. G. Khachaturyan, Sov. Phys. Solid State, 9, 2249 (1968).

21. P. Hirsch, A. Howie, R. B. Nicholson, D. W. Pashley, and M. J. Whelan, "Electron Microscopy of Thin Crystal", Robert E. Krieger Publishing Co., Inc. (1977).

22. P. A. Beaven and E. P. Butler, Acta Metall. 28, 1349 (1980).

23. A. G. Khachaturyan and G. A. Shatalov, Sov. Phys. Solid State, 11, 118 (1969).

24. U. Dahmen, K. H. Westmacott, and G. Thomas, Acta Metall. 29, 627 (1981).

FIGURE CAPTIONS

1. Conceptualization of the transformation process.
2. Illustration of α and β angles.
3. Theoretical prediction and TEM observation of the habit shifted angles with aspect ratio change.
4. Aspect ratio changes of α'' particle during coarsening.
5. Schematic Kikuchi map of B.C.C.
6. Rosette Morphology of α'' precipitate seen in [111] beam direction; aged at 100°C for 10 min. and at room temperature for two months.
7. Rosette morphology in [319] zone axis; A precipitate is nearly edge-on; same aging conditions as with Fig. 6.
8. Rosette morphology in later stage, aged at 150°C, 100 min.; seen in: (a) [115], (b) [139], (c),(d) [111] beam directions. The difficult growth directions <102> is now projected as <112> on (111) plane.
9. Dark field image of edge-on α'' precipitate shows the habit plane shifts at early stage.
10. The habit plane shift phenomenon was observed in inclined direction [111] (a-c), and in edge-on direction (d-f).
11. Habit plane curved precipitate, aged at 150°C for 100 min. (a) B.F. in [001] zone axis, (b) D.F. from 020 precipitate diffraction spot, (c) the diffraction pattern shows the crystal structure of the habit shifted part is distorted from tetragonal structure. Schematic diffraction pattern is also given in (c).

12. The unshifted part A and shifted part B of α" precipitate in inclined direction. (a) Some precipitate remains on (001) habit, (b-f) the others shift their habit planes, (b) B.F., (c) D.F., (d) W.B.D.F. all in [389] beam direction, (e) in [011], (f) in [012] beam directions.

TABLE I. Calculation result of the shifted angles with aspect ratio change in α" precipitate.

Z_o	R_o	$K=2R_o/Z_o$	θ	Orientation of Habit Normal
10.0	50.0	10.0	0	[001]
9.5	51.299	10.8	0	[001]
9.25	51.9875	11.24	0	[001]
9.2	52.1286	11.34	0	[001]
9.1	52.4142	11.52	1.65°	[0.029,0,0.996]
9.0	52.704	11.71	2.95°	[0.051,0,0.999]
7.5	57.735	15.38	10.35°	[0.180,0,0.984]
5.0	70.71	28.28	15.94°	[0.275,0,0.962]
2.5	100.00	80.00	19.47°	[0.333,0,0.943]
0	---	∞	22.5°	[0.382,0,0.924]

TABLE II. Dimensional parameters for α" particles.

Source	D(Å)	Z(Å)	K	$\sqrt{D}$	$\frac{K}{\sqrt{\ln K-1}}$
Wagner and Brenner	66	7.17	9.2	8.12	8.33
	90	8.11	11.1	9.49	9.35
	126	8.63	14.6	11.22	11.26
	225	9.62	23.4	15.00	15.90
	256	10.00	25.6	16.00	17.09
Keh and Wriedt	900	25	36	30.00	22.4
	1000	31	32	31.62	20.38
	1300	33	39	36.06	23.90
	2500	51	49	50.00	28.81
	3000	52	58	54.77	33.15
Abiko and Imai	1500	50	30	38.73	19.36
	8000	100	80	89.44	43.5
Direct TEM Measurement	1700	20	85.0	41.23	45.81
	2000	25	80.0	44.72	43.50
	3400	40	85.0	58.3	45.81
	4200	42	100.0	64.80	52.67
	4970	50	99.4	70.50	52.39
	15500	122	127.05	124.50	64.80
	18000	136	132.35	134.16	67.14

TABLE III. The observed shift angles with the dimensional parameters change of α" particles.

$2R_o$ (Å)	Z(Å)	K	θ_o
1000	-	-	12°
1700	20	85	15°
3000	_	_	15°
15500	122	127	19°

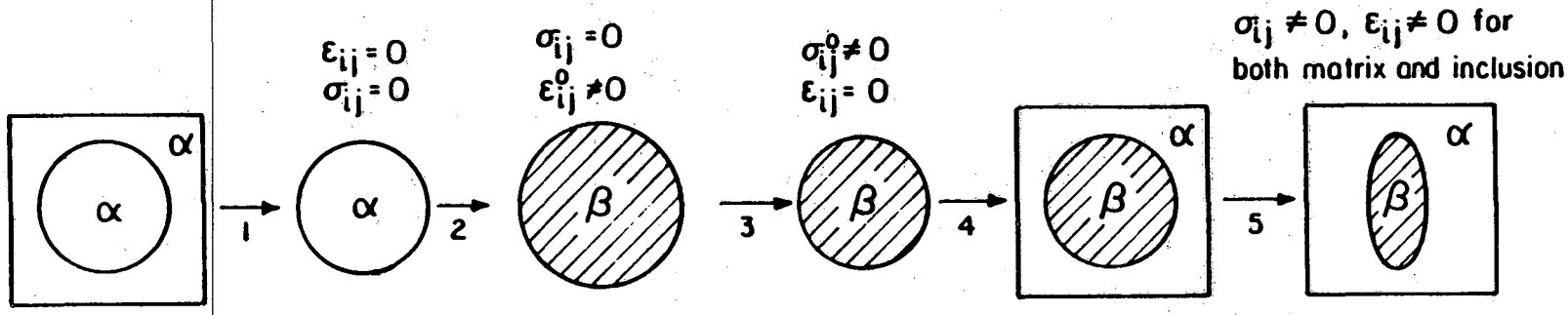

Figure 1

XBL 785-5008

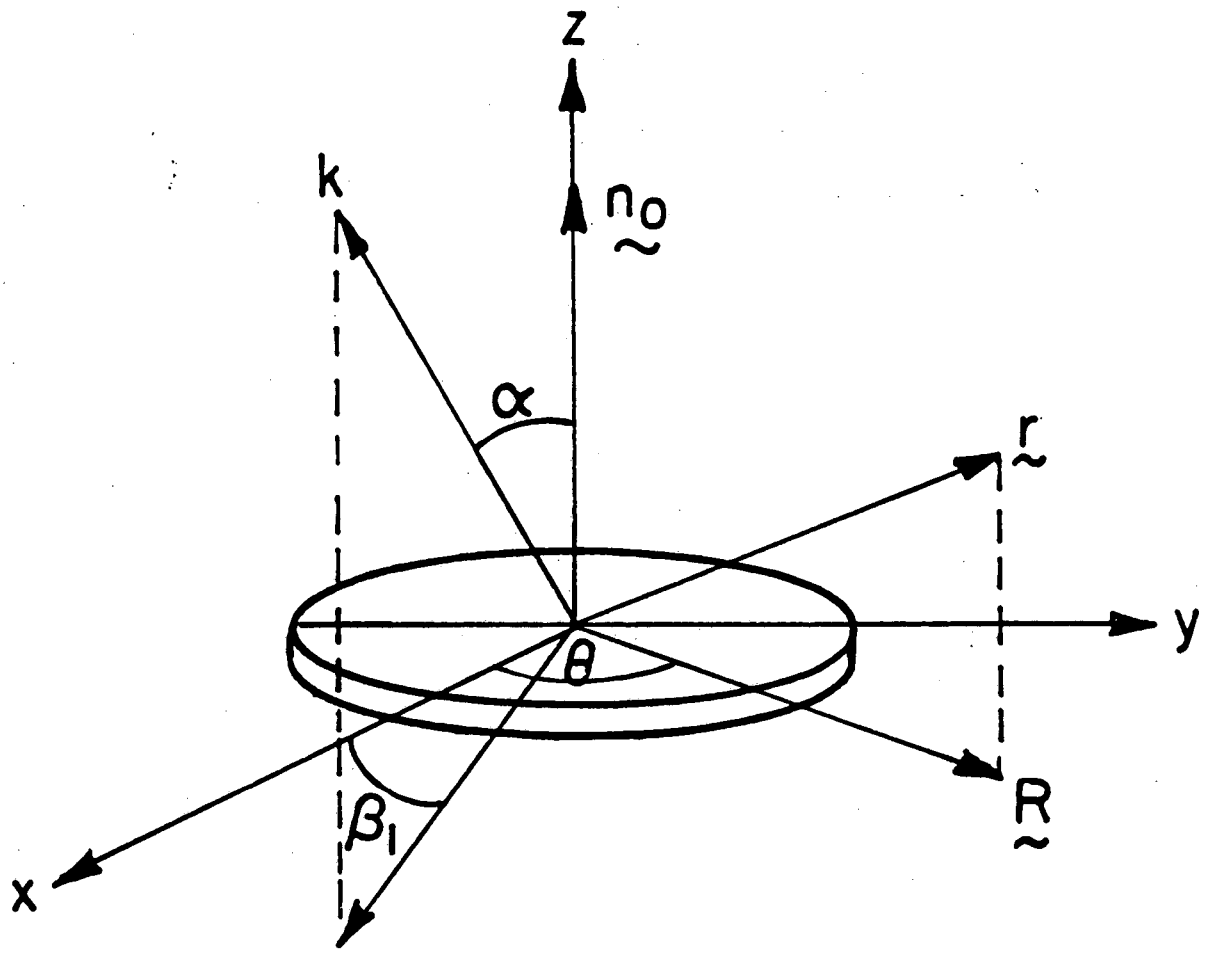

Figure 2

XBL785-5009

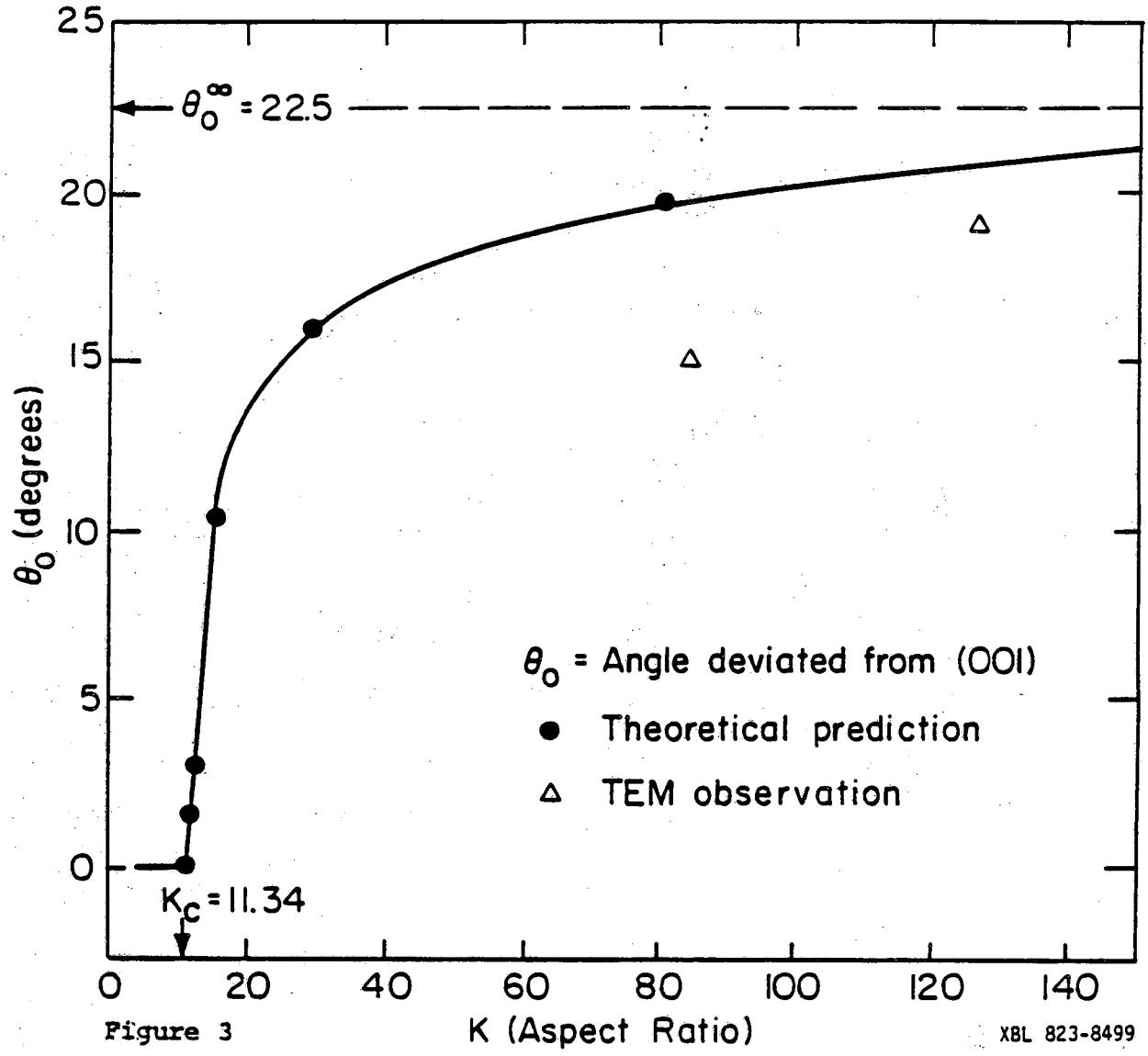
25
20
15
10
5
0
$\theta_0^\infty = 22.5$
θ_0 (degrees)
$K_c = 11.34$
0
20
40
60
80
100
120
140
K (Aspect Ratio)
θ_0 = Angle deviated from (001)
Theoretical prediction
TEM observation
XBL 823-8499

Figure 3

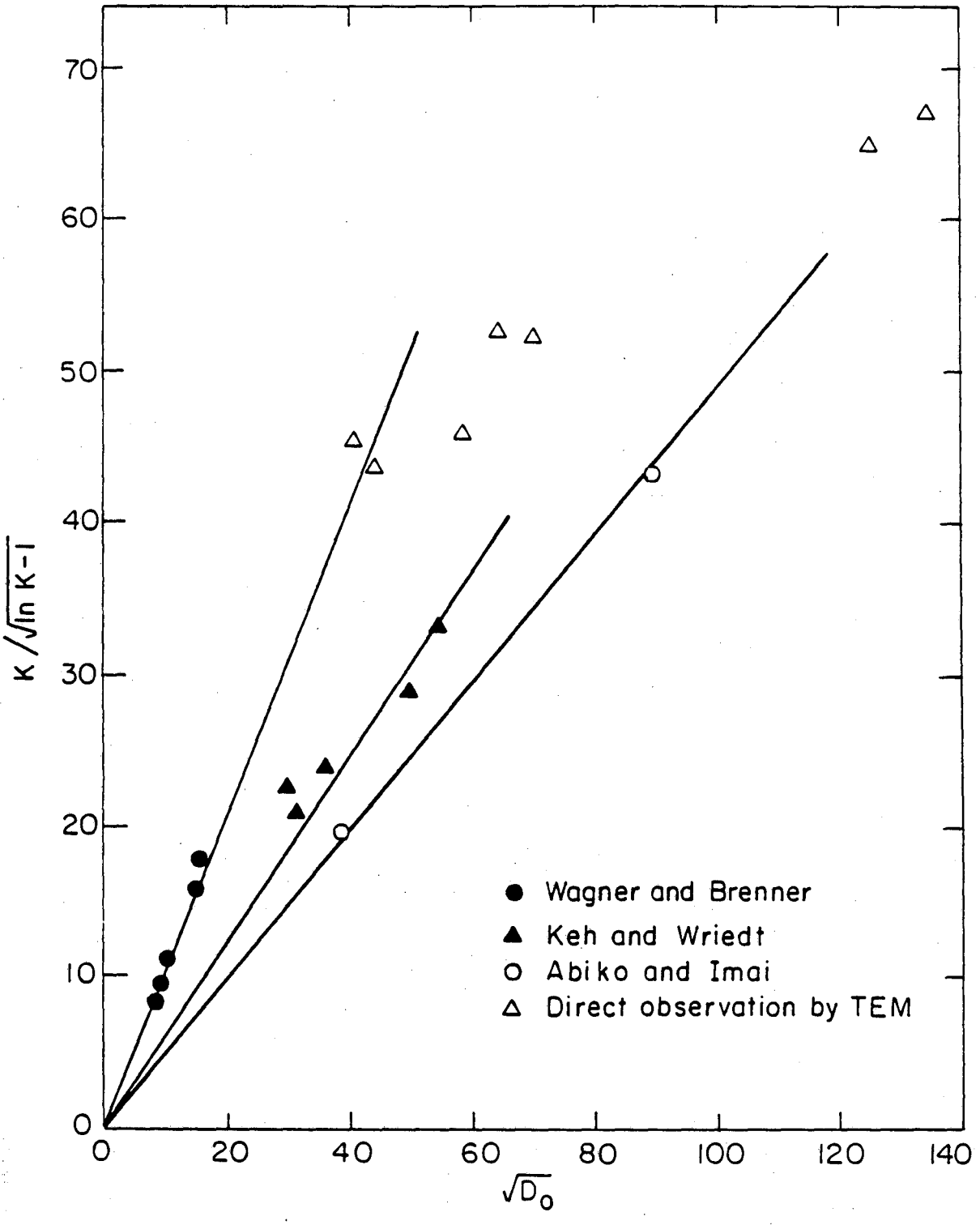

Figure 4

XBL 823-5328

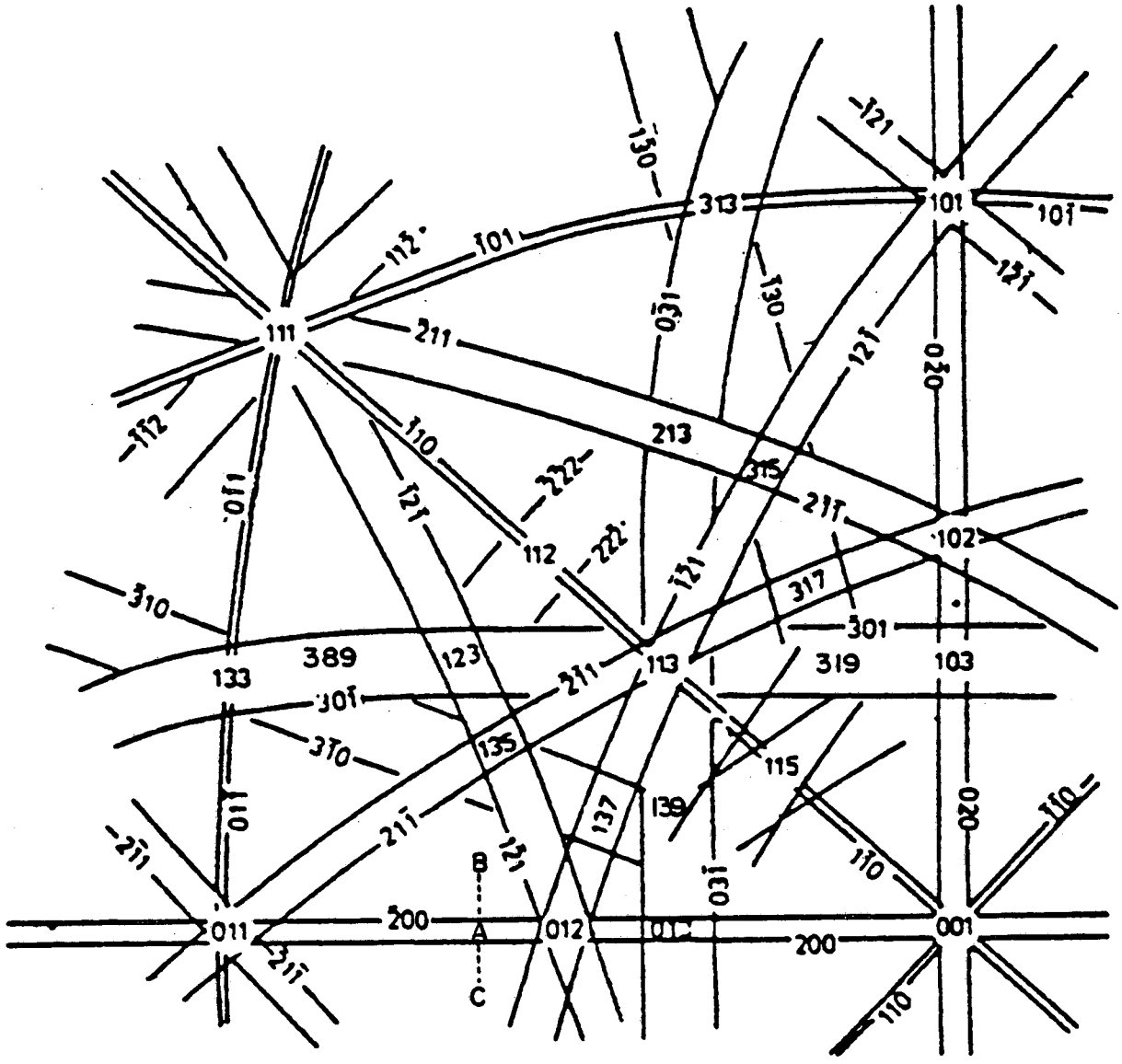

Figure 5

XBL 823-8759

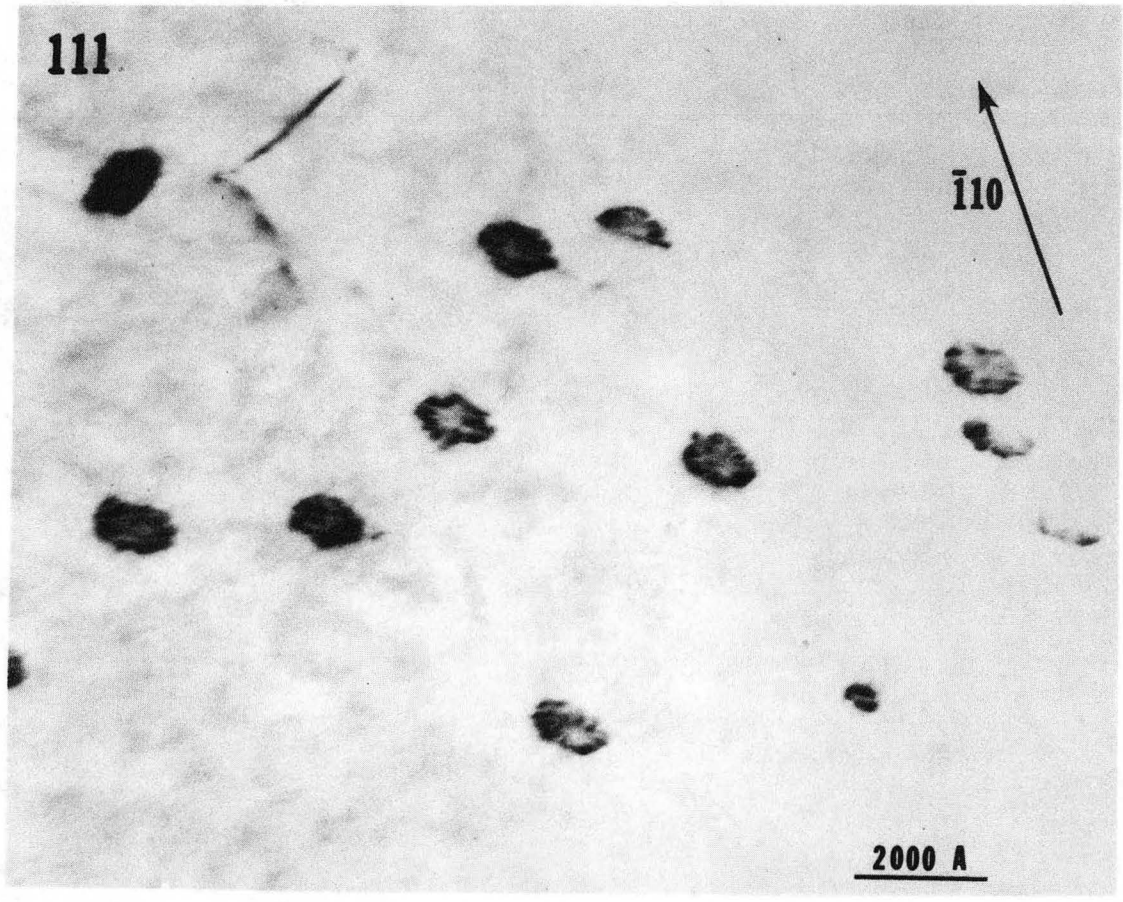

Figure 6

XBB 813-2952

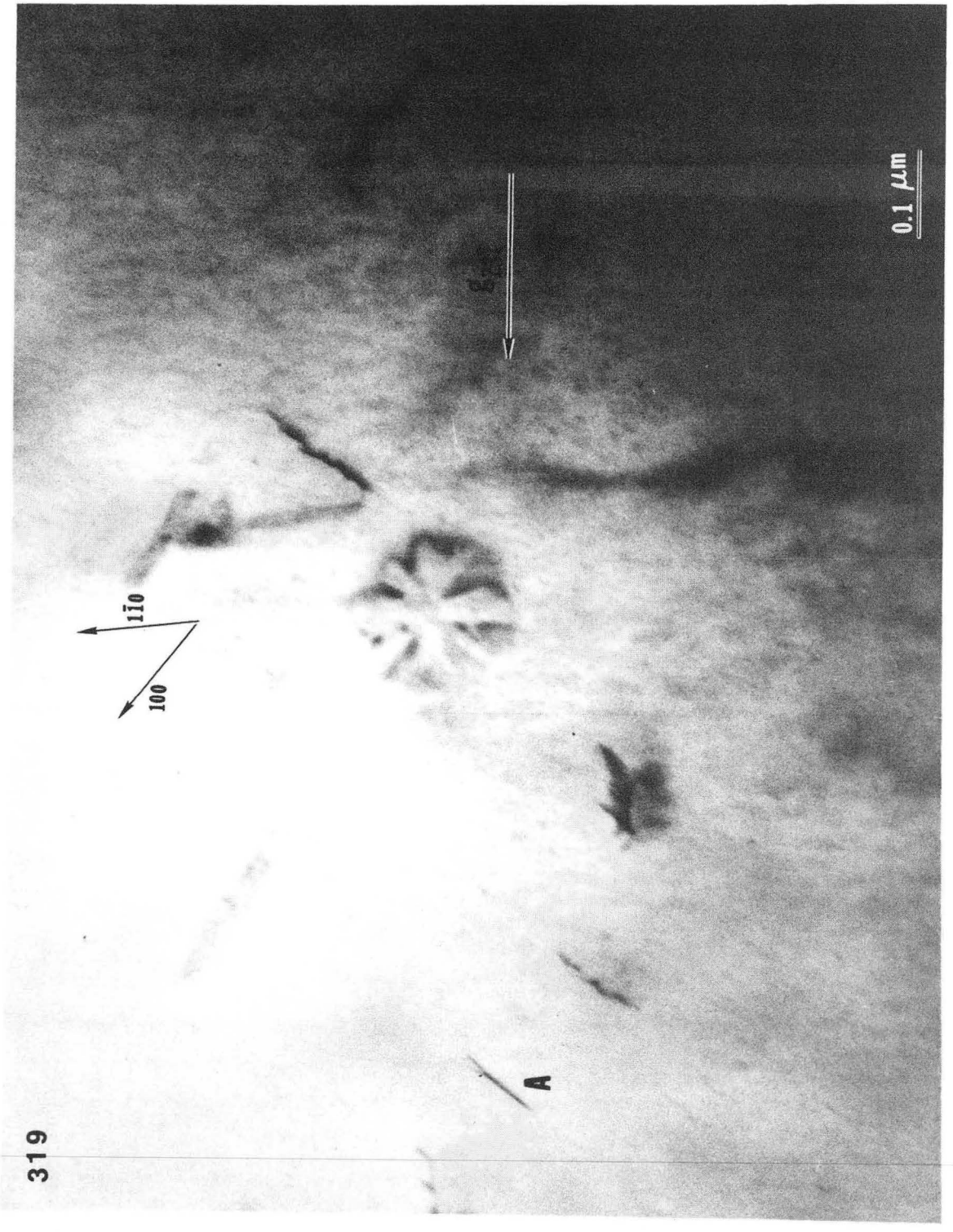

Figure 7

XBB 823-1779

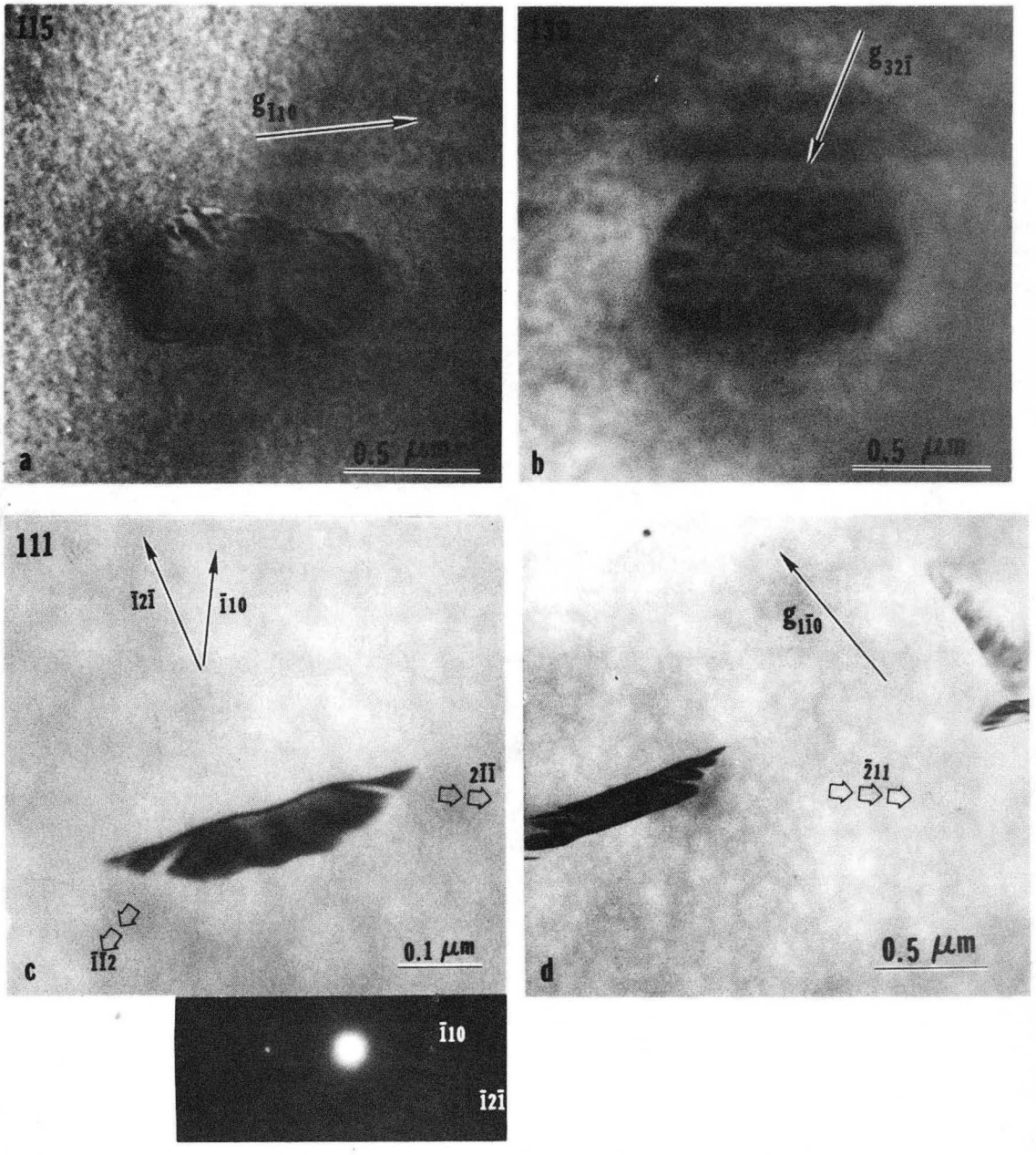

Figure 8

XBB 823-1776

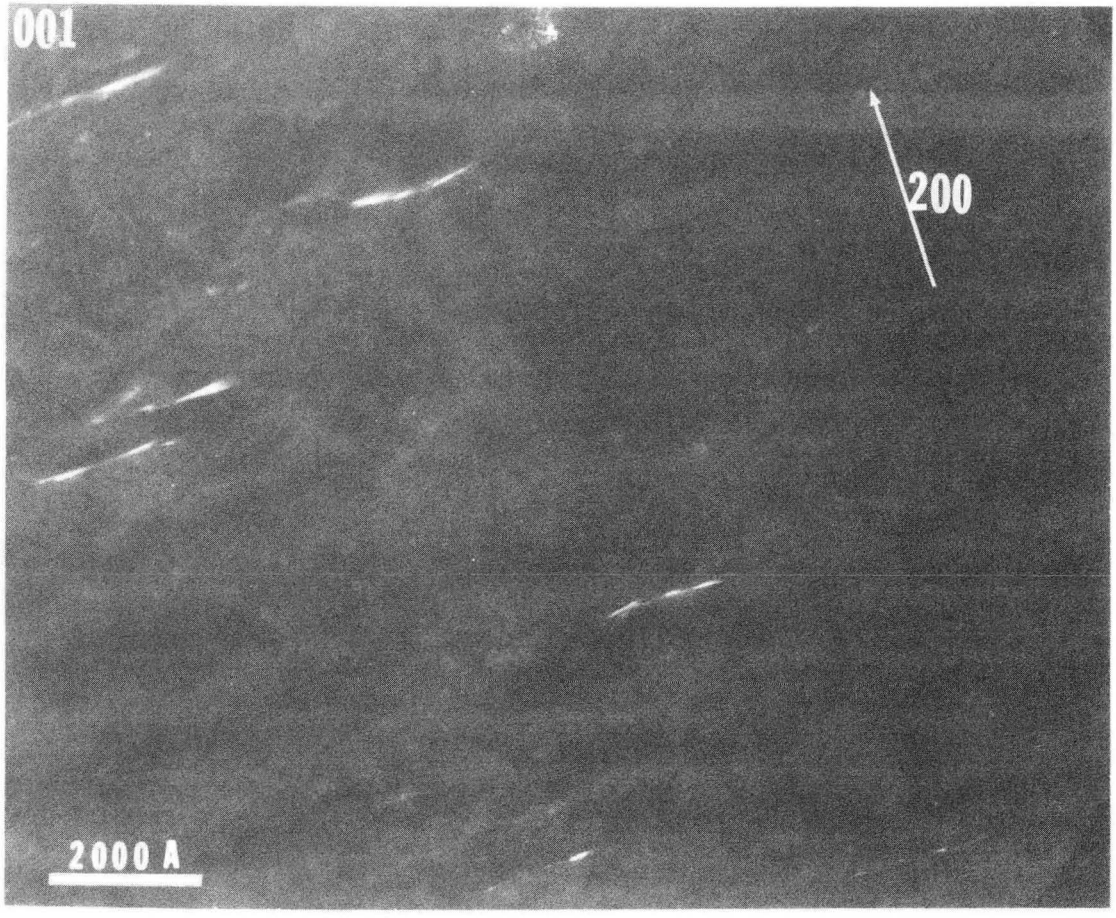

Figure 9

XBB 813-2954

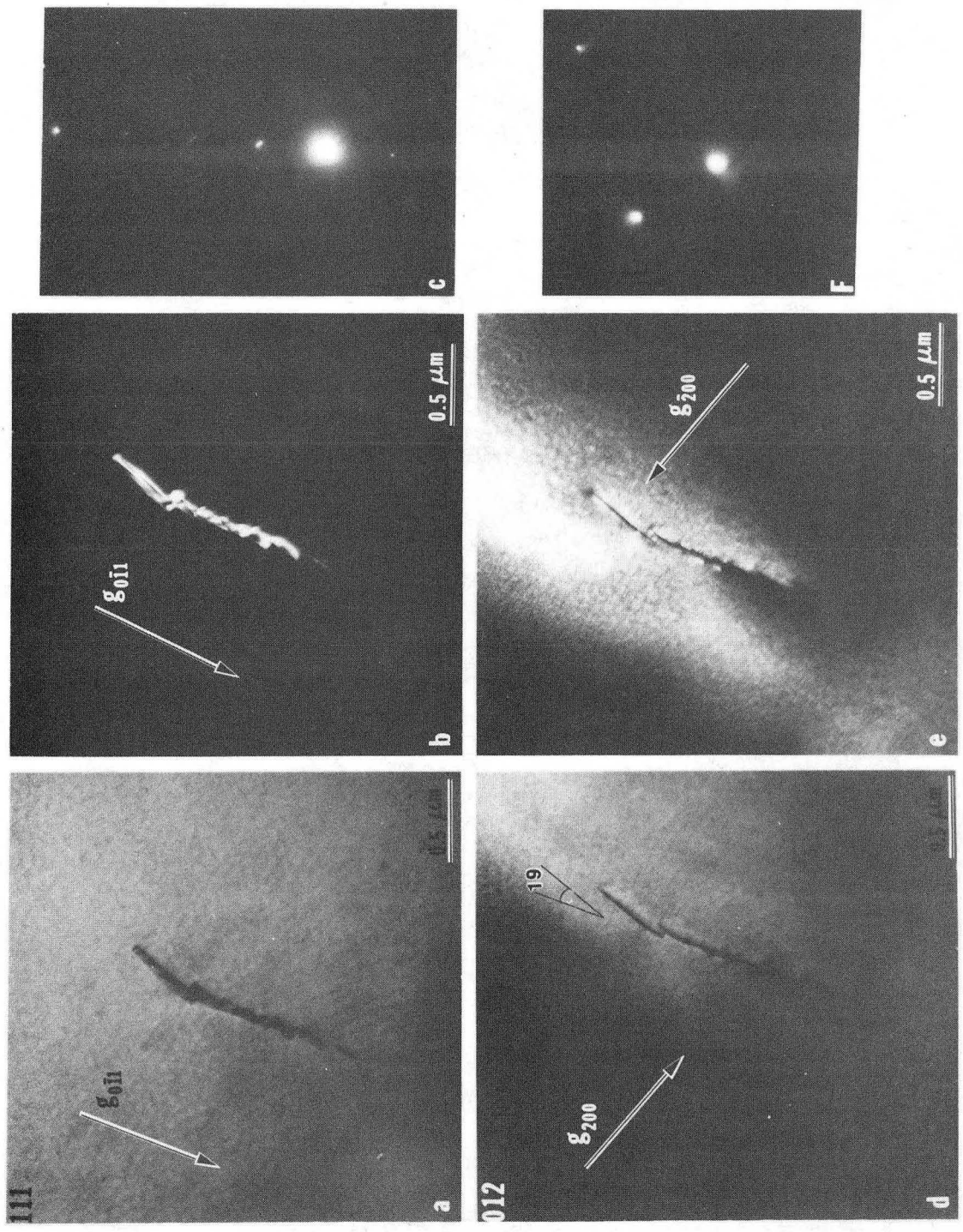

Figure 10

XBB 823-1775

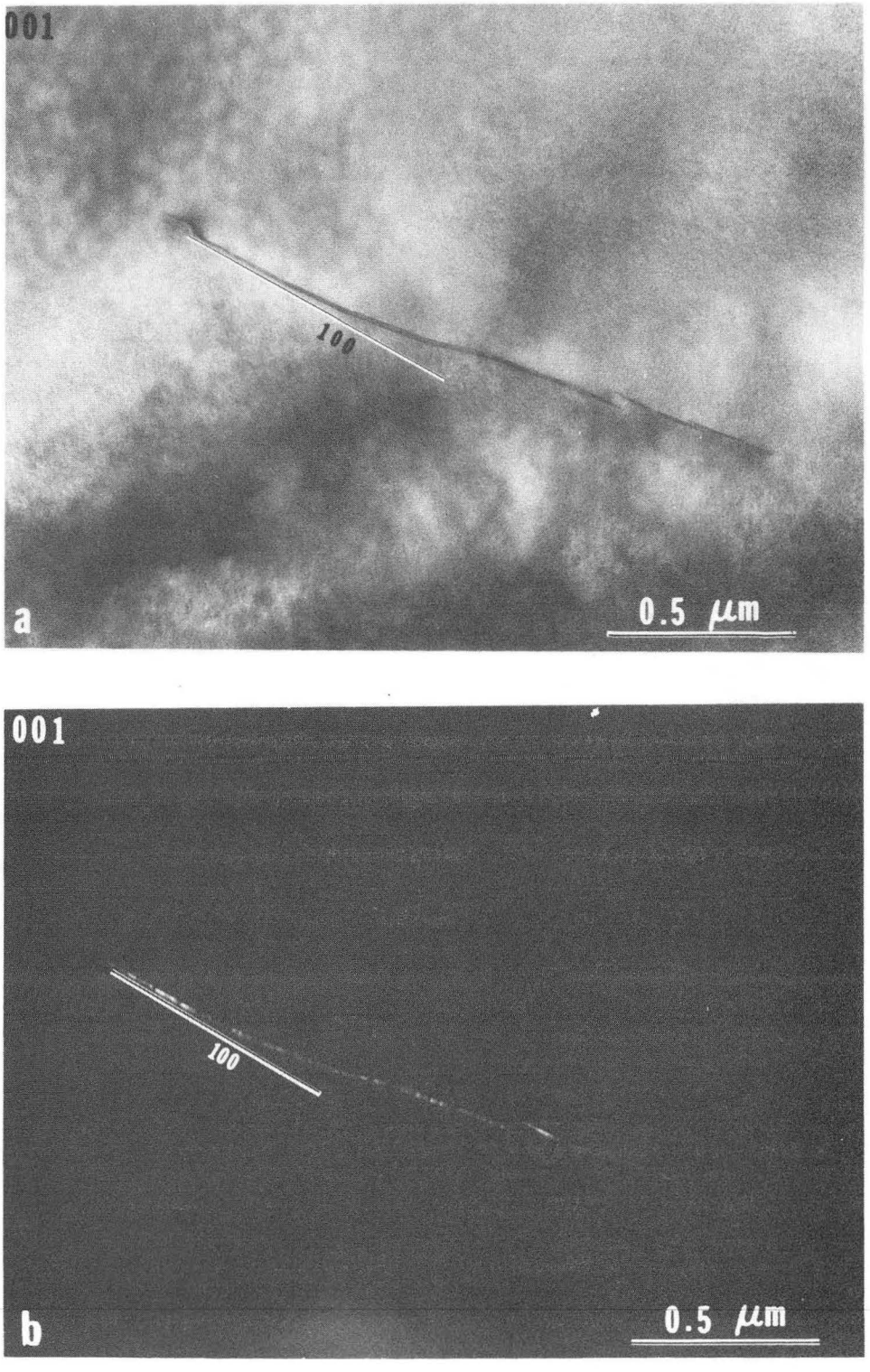

Figure 11

XBB 823-1778

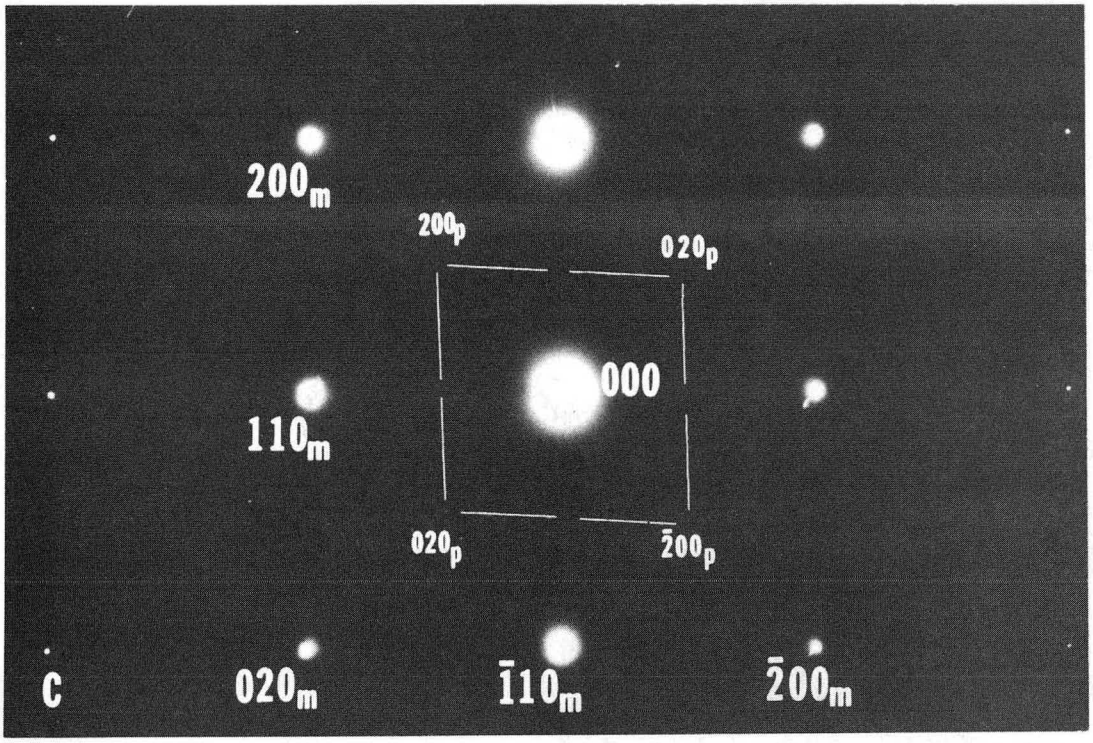

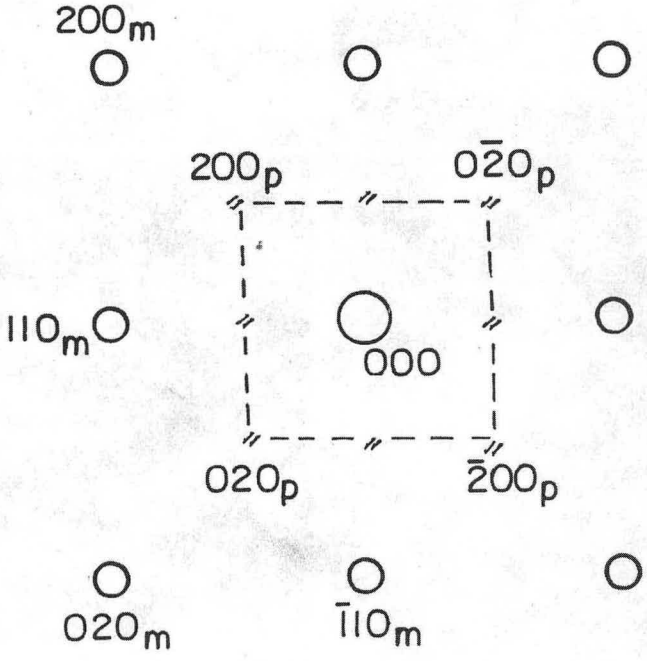

Figure 11c

XBB 823-1916

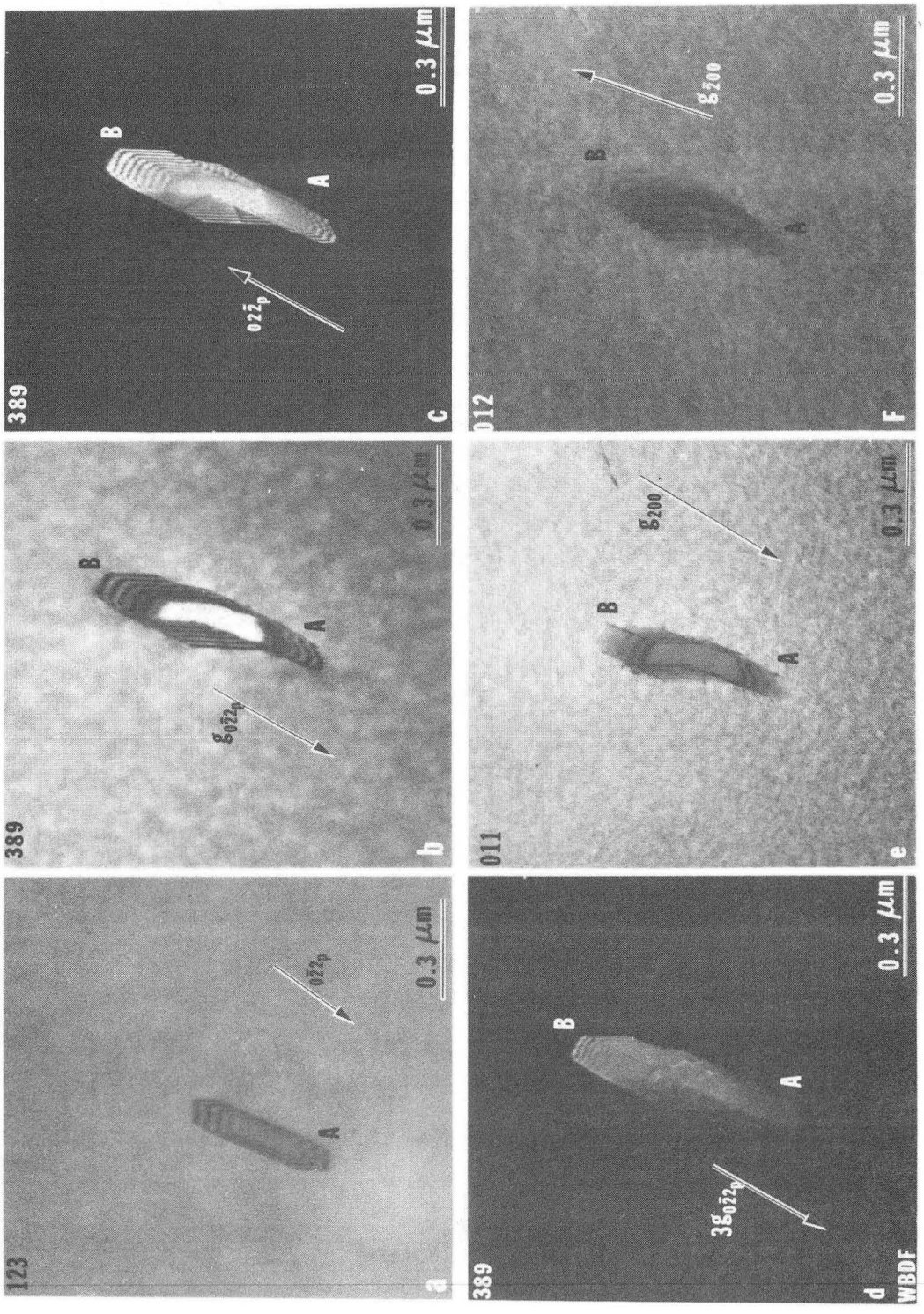

Figure 12

XBB 823-1777

TECHNICAL INFORMATION DEPARTMENT
LAWRENCE BERKELEY LABORATORY
UNIVERSITY OF CALIFORNIA
BERKELEY, CALIFORNIA 94720